Paper: ASAT-13-CT-31

13th International Conference on
AEROSPACE SCIENCES & AVIATION TECHNOLOGY,
ASAT- 13, May 26 – 28, 2009, E-Mail: asat@mtc.edu.eg
Military Technical College, Kobry Elkobbah, Cairo, Egypt
Tel : +(202) 24025292 – 24036138, Fax: +(202) 22621908

Flight Simulation Model for Small Scaled Rotor Craft-Based UAV

A. El-Saadany*, A. Medhat* and Y. Z. Elhalwagy*

Abstract: Many control system designs have been developed for controlling the dynamic process of aerospace vehicles. Yet, among those designs, few are readily suitable for applying. Moreover, most of the applicable aerospace control designs are built through flight tests that perform real processes on available real vehicles. The need to use real vehicles in the control design cycle poses a high risk and is prohibitively cost. To solve this problem, a real-time simulation concept that employs cheap, practical, and rapid-to-build modular hardware, which can simulate a nearly real process in lab's environment, is proposed in this research work. This paper elaborated the integration of nonlinear model for small scale helicopter, "Yamaha R-50", with the sensors, servos, and wind models into a modular Simulink model. The Simulink model performed a real-time computing process and behaved like the represented helicopter dynamic system. The overall scheme of flight simulation can play a significant role in the efficient control system design for aerial vehicles.

Keywords: Small scale helicopter, servo, INS, GPS.

1. Nomenclature

Latin variables

A	Rotor disk area	I_{CR}	Inertial momentum of the control rotor
a	Two-dimensional constant lift curve slope	K_{MR}	Swash plate linkage gain
A_{MR}	Lateral main rotor pitch input	K_{CR}	Control rotor linkage gain
A_{SP}	Lateral swash plate pitch input	m	Mass of helicopter
B_{MR}	Longitudinal main rotor pitch input	Q_{MR}	Main rotor drag
B_{SP}	Longitudinal swash plate pitch input	R	Main rotor radius
c	Mean blade length	T_{MR}	Main rotor thrust
F	Force vector $[f_x \quad f_y \quad f_z]^T$	T_{TR}	Tail rotor thrust
g	Gravitational acceleration	V	Translatory velocities vector $[u \quad v \quad w]^T$
I	Inertia matrix		

* Egyptian Armed Forces

Greek variables

β_{1c}	Longitudinal flapping angle	θ_{0tr}	Tail rotor collective pitch angle
β_{1s}	Lateral flapping angle	θ_{tw}	Blade twist angle
$\beta_{CR,1c}$	Control rotor longitudinal tilt angle	ω	Angular velocity vector $[p \quad q \quad r]^{T}$
$\beta_{CR,1s}$	Control rotor lateral tilt angle	τ	Torque vector $[L \quad M \quad N]^{T}$
Θ	Vector of Euler angles $[\varphi \quad \theta \quad \psi]^{T}$	Ω	Main rotor speed (RPM)
θ_{0}	Main rotor collective pitch angle	ρ	Density of air

Scripts

$\mathcal{P}$	Rotation matrix used to map velocities between two different frames

2. Introduction

Flight simulation in aerospace engineering is increasingly being required for the design as it becomes a very beneficial tool for exploring a variety of outcomes without taking a risk of losing any real vehicles. An advantage of this simulation tool is that for a successful controller test, the mathematical helicopter model needs to be replaced by the real helicopter. This paper describes the development and use of simulation tools for a small scale helicopter, “Yamaha R-50”, whose dimensions and physical characteristics are shown in Fig. 1 and Table 1, respectively (based on R-50 operating manual). The mathematical model of the helicopter will first be described in limited detail, which consists of servos, a nonlinear model of the small scale helicopter, “Yamaha R-50”, and internal on-board sensors.

Table 1 Yamaha R-50 physical characteristics

Rotor speed	850 rpm
Tip speed	449 ft/s
Total length	3.6 m
Dry weight	97 lb
Instrumented	150 lb
Flight autonomy	30 minute
It can carry a payload up to	20 Kg

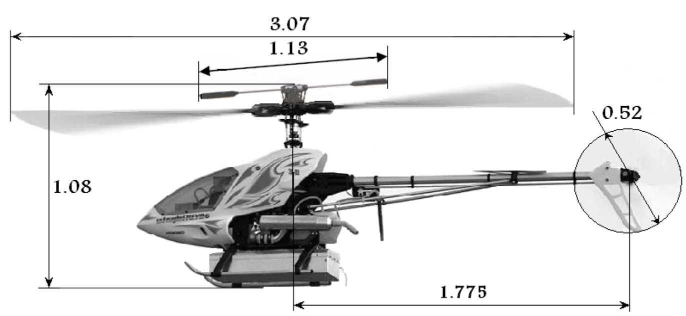

Fig. 1 Yamaha R-50 dimensions (meter).

The accuracy of the mathematical model of the helicopter dynamic becomes the major concern in the flight simulation. The better the mathematical model of the whole system and all important aspects such as, disturbances, noise, and time delays, the easier is the transition from simulation to real flight. Then, the development of a simulation tool described, including a variety of configurations that have been used. The paper terminated by conclusion and discussion.

3. Helicopter Mathematical Model

The helicopter is specified in regards to other transportation means, not just by its structure but also by its motion possibilities. The helicopter can move vertically, float in the air, turn in place, move forward and lateral, and can perform these movements in combinations.

Helicopter dynamics modeling has always been a challenging task and that result of a high degree of dynamic complexity, cross-coupling between the many transmission coordinates and many sources of vibration. In addition, most of modeling and simulation programs do not contain on models for rotor crafts. The complexity of helicopter flight dynamics makes modeling itself difficult, and without a good model of the flight-dynamics, the flight-control problem becomes inaccessible to most useful analysis and control design tools.

There are two approaches to obtain such a model, first principle modeling and system identification [1]. First principle modeling is using physical principles and laws to describe systems behavior. But the system identification is an effective method of obtaining a model from experimental data, Problems with the system identification method is that the identified model is well suited to flight control and simulation applications only in the conditions present during the flight-data collection [2]. In this paper, the model development will primarily use first principle method, where after parameter identification will be used to determine parameters that can't be measured directly.

Fig. 2 shows the components that make up the helicopter model. The modeling progression will follow the block diagram from left to right. Here a short description of the input to the block and the output from the block will follow.

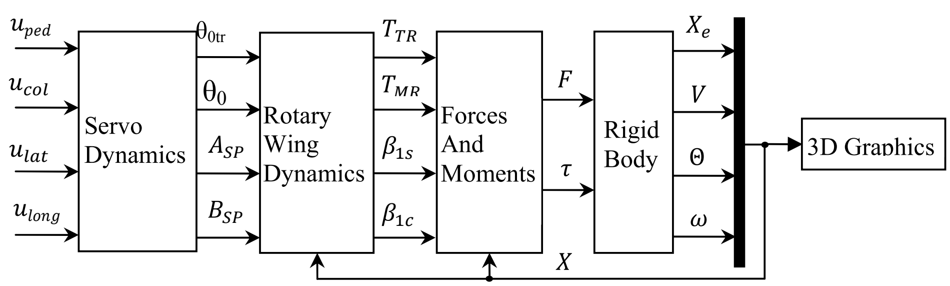

Fig. 2 Helicopter model block diagram.

3.1 Servo Dynamics:

The four servos are controlling the pitch angle of the blades of either the main or tail rotor. All servos were identical, and were modeled as an ideal second order nonlinear system. The saturation limits of the servo are included. These saturation limits are based on pitch operating range data from real world helicopters [3] and listed in Table 2.

The four inputs u_{ped}, u_{col}, u_{lat} and u_{long} represent pedal, collective, lateral and longitudinal pitch input, respectively. These inputs are a pulse-width modulation (PWM) signals from the receiver controlled either by the pilot (in piloted flight) or the controlling computer (when operating autonomously). The output is the attitude of the swash plate. This means the tilt of the swash plate in longitudinal B_{SP} and lateral direction A_{SP}, and position of the swash plate on the shaft which is proportional to the collective pitch θ_0. The signal θ_{0tr} is used to control the tail rotor collective pitch.

Table 2 Estimated servos operating range

Input	Range
u_{lat}	$\pm\,0.175\,rad$
u_{long}	$\pm\,0.175\,rad$
u_{col}	$\pm\,0.175\,rad$
u_{ped}	$\pm\,0.35\,rad$

3.2 Rotary Wing Dynamics:

This block describes the non trivial task of modeling the rotor dynamics, the block diagram shown in Fig. 4 shows a graphical description of how the elements contained in rotary dynamics, interact. A short description of each element will follow.

3.2.1 Thrust model

This model is designed to determine the main and tail rotor thrust magnitudes (T_{MR} and T_{TR} respectively) as a function of the pitch inputs θ_0 and θ_{0tr} using blade element and momentum theory [4]. The thrust magnitudes are also dependent on the 4 translator movement of the helicopter and the attitude of the helicopter body. The direction of the thrust is defined by the lateral and longitudinal flapping angels (β_{1s} and β_{1c} respectively), which are functions of the swash plate tilting. The expressions for β_{1s} and β_{1c} are also influenced by factors such as 4ranslator movement and rotation of the helicopter body.

3.2.1.1 Main Rotor Thrust Equations:

The thrust generated by the main rotor can be described by the following equations:

$$\hat{V}^2 = \left(u\cos(\beta_{1c})\right)^2 + \left(v\cos(\beta_{1s})\right)^2 + \left(w\sin(\beta_{1c})\sin(\beta_{1s})\right)^2 \tag{1}$$

$$\omega_r = w\cos(\beta_{1c})\cos(\beta_{1s}) + u\sin(\beta_{1c}) - v\sin(\beta_{1s}) \tag{2}$$

$$v_i = \sqrt{-\frac{\hat{V}^2 + \omega_r(\omega_r - 2v_i)}{2} + \sqrt{\left(\frac{\hat{V}^2 + \omega_r(\omega_r - 2v_i)}{2}\right)^2 + \left(\frac{T}{2\rho A}\right)^2}} \tag{3}$$

$$T_{MR} = \frac{\rho}{4}\Omega^2 R^3 b\,c\,a\left(\frac{2}{3}\left(\theta_0 + \frac{3}{4}\theta_{tw}\right) - \left(\frac{v_i - \omega_r}{\Omega R}\right)\right) \tag{4}$$

where v_i is the induced wind velocity.

3.2.1.2 Tail Rotor Thrust Equations:

The main purpose of the tail rotor thrust T_{TR} is to compensate the moment which are generated by the main rotor about the z-axis of the BF. And for simplification, the tail rotor thrust was calculated by cancelling out the moment generated by the main rotor drag.

$$T_{TR} = \frac{{}^{b}f_{x,MR}\, y_m + {}^{b}f_{y,MR}\, l_m - Q_{MR}\cos(\beta_{1c})\cos(\beta_{1s})}{l_t} + u_{ped} \tag{5}$$

3.2.2. Flapping

The lateral and longitudinal inputs to the swash plate are controlled by the pilot, and fed to both the main rotor and the control rotor. A part of the input is fed directly to the main rotor, while the other part of the input is fed to the main rotor through the control rotor. The mixing of the input is illustrated in Fig. 4. The inputs from the swash plate, A_{SP} and B_{SP}, result in lateral and longitudinal blade flapping on the main rotor denoted β_{1s} and β_{1c}. The control rotor has a mechanical linkage gain to the main rotor denoted K_{CR}. The input results in a flapping motion of the control rotor of which the angles are expressed by $\beta_{CR,1s}$ and $\beta_{CR,1c}$. The mechanical linkage gain from the swash-plate to the main rotor is defined as K_{MR}. The mixer system from swash plate input to main rotor input is described as:

$$\begin{aligned} A_{MR} &= K_{MR}A_{SP} + K_{CR}\beta_{CR,1s} \\ B_{MR} &= K_{MR}B_{SP} + K_{CR}\beta_{CR,1c} \end{aligned} \tag{6}$$

3.2.2.1 Control Rotor Flapping

A small scale helicopter has much faster dynamics than a full sized counter part and this can pose a problem for the human pilot. This problem is corrected by using a control augmentation in the form of a control rotor. Fig. 3 shows the connection between the fuselage and the rotor disk. The control rotor consists of a teetering rotor mounted on the same shaft as the main rotor.

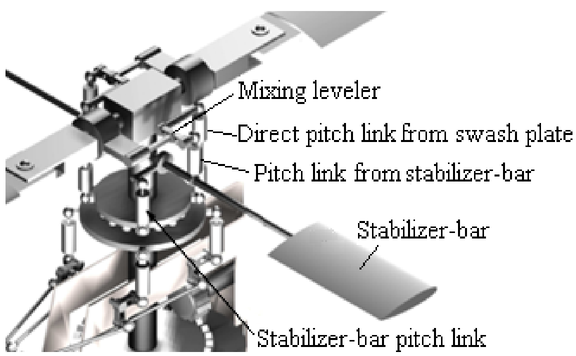

Fig. 3 Drawing of stabilizer-bar.

It is made from a steel rod with small paddles at both ends acting as small rotor blades. By teetering rotor it is implied that the control rotor is free to flap without restraint. From the swash plate the control rotor receives longitudinal and lateral inputs, much like the main rotor. But unlike the main rotor it does not receive any collective input, and thus do not produce any lift which would result in a coning angle of the control rotor.

The equation given for the control rotor flapping angel rate in the lateral direction is:

$$\dot{\beta}_{CR,1s}(t) = \frac{1}{4}\Omega T_1 A_{SP}(t) - p(t) - \frac{1}{4}\Omega T_2 q(t) - \frac{1}{2}\Omega\, \beta_{CR,1s}(t) - \frac{1}{4}\Omega T_1 \dot{\beta}_{CR,1c}(t) - \frac{\ddot{\beta}_{CR,1c}(t)}{2\Omega} \tag{7}$$

and in the longitudinal direction is:

$$\dot{\beta}_{CR,1c}(t) = \frac{1}{4}\Omega T_1 B_{SP}(t) + \frac{1}{4}\Omega T_2\, p(t) - q(t) + \frac{1}{2}\Omega\, \beta_{CR,1c}(t) + \frac{1}{4}\Omega T_1\, \dot{\beta}_{CR,1s}(t) + \frac{\ddot{\beta}_{CR,1s}(t)}{2\Omega} \tag{8}$$

where:

$$T_1 = \gamma\left(-\frac{1}{4} + \frac{R_{CR,P}^4}{4R_{CR}^4}\right),\ \ T_2 = \gamma\left(-\frac{1}{4\Omega} + \frac{R_{CR,P}^4}{4\Omega R_{CR}^4}\right), \tag{9}$$

and

$$\gamma = \frac{\rho c\, a\, R_{CR}^4}{I_{cr}} \tag{10}$$

where:

I_{CR} is the inertial momentum of the control rotor

$R_{CR,P}$ is the distance from the center of the rotor hub to the beginning of the paddle

R_{CR} is the distance from the center of the rotor hub to the end of the control rotor as shown in Fig. 5.

The resulting equations describe a MIMO system where $\beta_{CR,1s}$ and $\beta_{CR,1c}$ are the outputs and the inputs are the shaft motions (p, q) and swash plate tilt angles (A_{SP}, B_{SP}). There is also a coupling between longitudinal and lateral flapping which can be seen in the two last terms in both flapping equations. This coupling is a result of the gyroscopic moments.

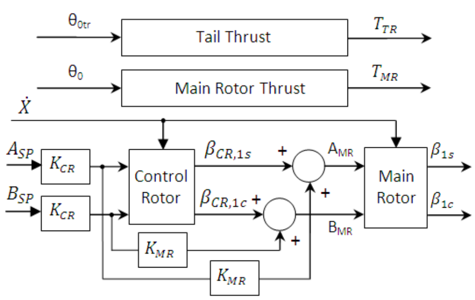

Fig. 4 Block diagram of rotary wing model.

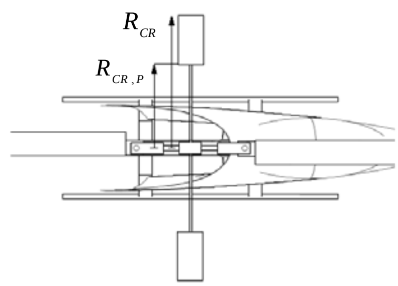

Fig. 5 Control rotor paddles.

3.2.2.2 Main Rotor Flapping

Giving cyclic input, A_{MR} and B_{MR} allows the tip path plane (spanned by the tip of the rotor blades) to flap or tilt in a longitudinal or lateral direction. This directing of the thrust vector is the basis for controlling a helicopter. The main rotor flapping section derives a quasi steady state model to describe this behavior. By quasi steady state it is implied that the equations do not account for the transient dynamics of the main rotor. This is because the main rotor is effectively governed by the control rotor input [5]. The main rotor in this paper is teetering rotor with no hinge offset. The equation given for the flapping angel in the lateral direction is:

$$\begin{aligned}\beta_{1s}(t) = \frac{3.06\cdot 10^{-7}}{\pi^2}\big(&-2456.91 A_{MR}\ {}^b v^2(t) + 3.263\cdot 10^6\,\pi^2 A_{MR} - 1637.94\, B_{MR}\ {}^b u(t)\ {}^b v(t)\, v_i - 4.67\cdot 10^5\,\pi\, p(t) \\ &+ 3275.88 v_i - 1.94\cdot 10^5\,\pi\, u_{col}(t)\ {}^b v(t) - 1.12\cdot 10^5\,\pi\, q(t) + 818.969\ {}^b u^2(t)\, A_{MR}\big)\end{aligned} \tag{11}$$

and in the longitudinal direction is:

$$\begin{aligned}\beta_{1c}(t) = \frac{3.06\cdot 10^{-7}}{\pi^2}\big(&-3.263\cdot 10^6\, B_{MR}\,\pi^2 - 816.969\ {}^b v^2(t) B_{MR} - 2456.91\ {}^b u^2(t)\, B_{MR} + 1637.94 A_{MR}\ {}^b v(t)\ {}^b u(t) \\ &-1.13\cdot 10^5\,\pi p(t) - 4.67\cdot 10^5\,\pi\, q(t) - 1.95\cdot 10^5\,\pi\, u_{col}(t)\ {}^b u(t) - 3275.88\ {}^b u(t)\, v_i\big)\end{aligned} \tag{12}$$

3.3. Force and Moment Generating Process:

This block deals with the derivation of the equations, describing the forces and moments acting on the helicopter. The inputs being the flapping angles β_{1s} and β_{1c}, the thrust generated by the main rotor, T_{MR}, and tail rotor, T_{TR}. The outputs are a three dimensional force and moment vector described in the BF.

3.3.1 Forces

This section describes the translatory forces acting on the helicopter. The resulting force, ${}^{b}F$, stated in the Body Frame (BF), is decomposed along the three axes ${}^{b}f_x$, ${}^{b}f_y$, and ${}^{b}f_z$, these forces consist of:

${}^{b}F_{MR}$: Forces caused by the main rotor thrust

${}^{b}F_{TR}$: Forces caused by the tail rotor thrust

${}^{b}F_{g}$: Forces caused by the gravitational acceleration

$$
\begin{aligned}
{}^{b}F = \begin{bmatrix} {}^{b}f_x \\ {}^{b}f_y \\ {}^{b}f_z \end{bmatrix} &= {}^{b}F_{MR} + {}^{b}F_{TR} + {}^{b}F_{g} = \begin{bmatrix} -T_{MR}\sin(\beta_{1c}) \\ T_{MR}\sin(\beta_{1s}) \\ -T_{MR}\cos(\beta_{1s})\cos(\beta_{1c}) \end{bmatrix} + \begin{bmatrix} 0 \\ -T_{TR} \\ 0 \end{bmatrix} + \begin{bmatrix} -mg\sin(\theta) \\ mg\sin(\phi)\cos(\theta) \\ mg\cos(\phi)\cos(\theta) \end{bmatrix} \\
&= \begin{bmatrix} -T_{MR}\sin(\beta_{1c}) - mg\sin(\theta) \\ T_{MR}\sin(\beta_{1s}) - T_{TR} + mg\sin(\phi)\cos(\theta) \\ -T_{MR}\cos(\beta_{1s})\cos(\beta_{1c}) + mg\cos(\phi)\cos(\theta) \end{bmatrix}
\end{aligned}
\tag{13}
$$

3.3.2 Moments

This section describes the moments acting on the helicopter about the three axes $({}^{b}x, {}^{b}y, {}^{b}z)$. These moments are primarily caused by three components:

${}^{b}\tau_{MR}$: Moments caused by main rotor

${}^{b}\tau_{TR}$: Moments caused by tail rotor

${}^{b}\tau_{D}$: Counter-moment caused by drag on the main rotor

$$
{}^{b}\tau = \begin{bmatrix} {}^{b}L \\ {}^{b}M \\ {}^{b}N \end{bmatrix} = \begin{bmatrix} {}^{b}L_{MR} \\ {}^{b}M_{MR} \\ {}^{b}N_{MR} \end{bmatrix} + \begin{bmatrix} {}^{b}L_{TR} \\ {}^{b}M_{TR} \\ {}^{b}N_{TR} \end{bmatrix} + \begin{bmatrix} {}^{b}L_{D,MR} \\ {}^{b}M_{D,MR} \\ {}^{b}N_{D,MR} \end{bmatrix} = \begin{bmatrix} {}^{b}f_{y,MR}\,h_m + {}^{b}f_{z,MR}\,y_m + {}^{b}f_{y,TR}\,h_t + Q_{MR}\sin(\beta_{1c}) \\ -{}^{b}f_{x,MR}\,h_m + {}^{b}f_{z,MR}\,l_m - Q_{MR}\sin(\beta_{1s}) \\ -{}^{b}f_{x,MR}\,y_m - {}^{b}f_{y,MR}\,l_m - {}^{b}f_{y,TR}\,l_t + Q_{MR}\cos(\beta_{1c})\cos(\beta_{1s}) \end{bmatrix} \tag{14}
$$

where: Q_{MR} is the magnitude of the moment generated by the main rotor.

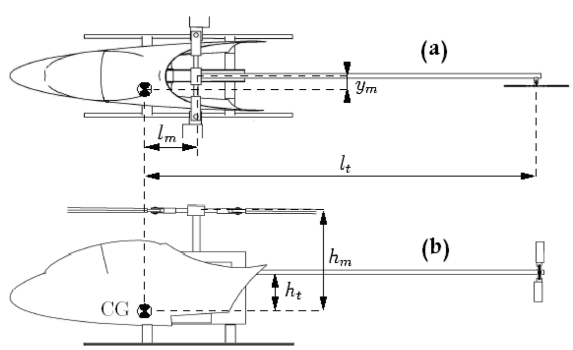

(a) Top view **(b) Side view**

Fig. 6 The distances used to calculate the moments generated by the main and tail rotor.

3.4 Rigid Body Dynamics:

Here the final equations that describe the translational and rotational movement of the helicopter are derived. For this purpose the helicopter is regarded as a rigid body.
There are four output vectors:

Position (X_e): relative to the Earth frame.

Velocity (V): relative to the Earth frame.

Euler angles (Θ): relative to spatial frame.

Euler rates (ω): relative to spatial frame.

Note: The spatial frame has its origin in the helicopter centre of mass and the same orientation as Earth frame.

There exists a dynamic coupling between the velocity and rotation of the helicopter and the forces and moments developed, and exerted on the helicopter. This coupling is indicated in the block diagram by the feedback of the state vector (X). This will be clarified in the following section.

The motion of the rigid body was described as follows:

$$\begin{bmatrix} {}^b\dot{V} \\ \dot{\Theta} \\ \dot{\omega} \end{bmatrix} = \begin{bmatrix} \frac{1}{m}\,{}^bF + \omega \times {}^bV \\ \mathcal{P}_{sb}(\Theta)\omega \\ \mathrm{I}^{-1}\left(M - \omega \times (\mathrm{I}\omega)\right) \end{bmatrix} \tag{15}$$

These equations can be expanded to:

3.4.1 Force equations:

$${}^b\dot{V} = \begin{bmatrix} {}^b\dot{u} \\ {}^b\dot{v} \\ {}^b\dot{w} \end{bmatrix} = \begin{bmatrix} \frac{{}^bf_x}{m} - {}^bwq + {}^bvr \\ \frac{{}^bf_y}{m} - {}^bur + {}^bwp \\ \frac{{}^bf_z}{m} - {}^bvp + {}^buq \end{bmatrix} \tag{16}$$

where:

${}^bF = \left[{}^bf_x, {}^bf_y, {}^bf_z\right]^{\mathrm{T}}$, ${}^bV = \left[{}^bu, {}^bv, {}^bw\right]^{\mathrm{T}}$, $\omega = [p, q, r]^{\mathrm{T}}$, and m is the mass of the helicopter.

3.4.2 Kinematics Equations:

$$\dot{\Theta} = \begin{bmatrix} \dot{\phi} \\ \dot{\theta} \\ \dot{\psi} \end{bmatrix} = \begin{bmatrix} p + \sin(\phi)\tan(\theta)q + \cos(\phi)\tan(\theta)r \\ \cos(\phi)q - \sin(\phi)r \\ \frac{\sin(\phi)}{\cos(\theta)}q + \frac{\cos(\phi)}{\cos(\theta)}r \end{bmatrix} \tag{17}$$

where: $\Theta = [\phi, \theta, \psi]^{\mathrm{T}}$ and $\omega = [p, q, r]^{\mathrm{T}}$

3.4.3 Moment Equations:

$$\dot{\omega} = \begin{bmatrix} \dot{p} \\ \dot{q} \\ \dot{r} \end{bmatrix} = \begin{bmatrix} (c_1 R + c_2 P)Q + c_3 L + c_4 N \\ c_5 PR - c_6\left(P^2 - R^2\right) + c_7 M \\ (c_8 P + c_2 R)Q + c_4 L + c_9 N \end{bmatrix} \tag{18}$$

where: $\omega = [p, q, r]^{\mathrm{T}}$, $\tau = [L, M, N]^{\mathrm{T}}$,

$$\begin{aligned} &\Gamma c_1 = \left(I_y - I_z\right) I_z - I_{xz}^2, \quad \Gamma c_2 = \left(I_x - I_y + I_z\right) I_{xz} \\ &\Gamma c_3 = I_z, \quad \Gamma c_4 = I_{xz}, \quad c_5 = \left(I_z - I_x\right)/I_y \\ &c_6 = I_{xz}/I_y, \quad c_7 = 1/I_y, \quad \Gamma c_8 = I_x\left(I_x - I_y\right) + I_{xz}^2 \\ &\Gamma c_9 = I_x, \quad \Gamma = I_x I_z - I_{xz}^2, \end{aligned} \tag{19}$$

and

$$\mathrm{I} = \begin{bmatrix} I_{xx} & 0 & -I_{xz} \\ 0 & I_{yy} & 0 \\ -I_{xz} & 0 & I_{zz} \end{bmatrix} \tag{20}$$

3.5 3D Graphics

As a result of the Simulink functionality, scopes can be attached to any signal point in the simulation environment or comparing several signal progressions over time. In addition an gauges that Display some of the model parameters on line with the simulation and also the VR-model that animates the helicopter movement. This is achieved by giving the VR-model a three dimensional vector containing coordinates of the position and a four dimensional vector for Eigen-axis rotation describing the attitude. Conversion of the Euler angles to the Eigen-axis rotation is performed by an S-function. A screen dump of the helicopter animation and the instruments are shown in Fig. 7 and Fig. 8.

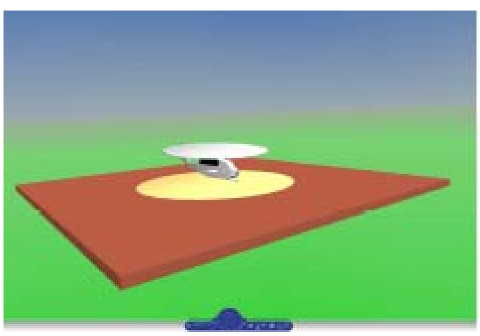

Fig. 7 Illustration of the helicopter Animation.

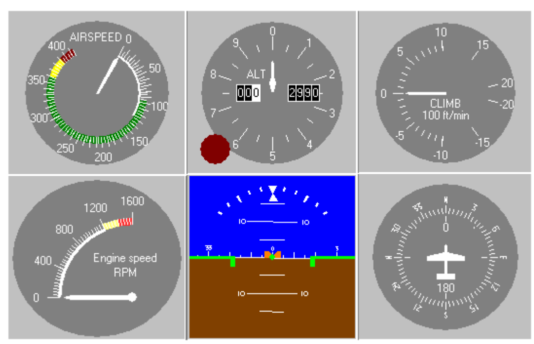

Fig. 8 Illustration of the gauges.

Fig. 9 shows the complete nonlinear helicopter model, and the modeling progression will follow the block diagram from left to right.

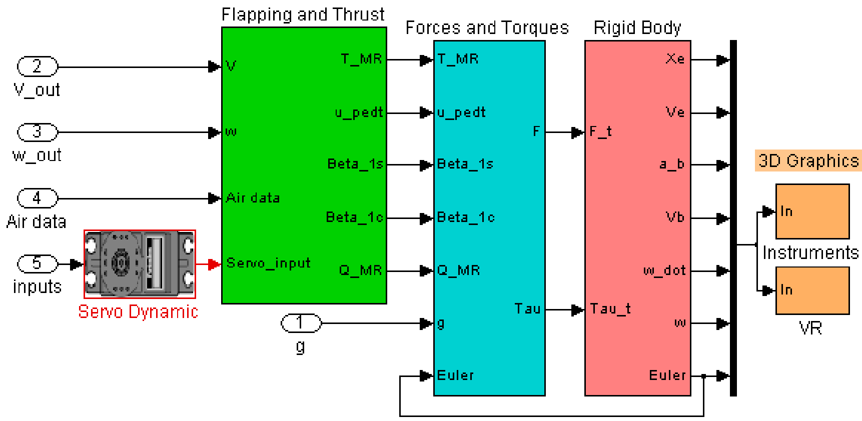

Fig. 9 The nonlinear model.

4. Avionics System

The avionics system is designed to allow logical information flow within the UAV system in accordance with control and navigation requirements. These avionics systems will be included the environment system and the navigation system.

4.1 Environment Model

The environment model is divided into five separate models. The first model calculates standard atmospheric parameters (temperature, air density, air pressure) at a given altitude. The second calculates Earth's gravity at a specific location. Steady wind model calculates wind magnitude at a given level. The calculations are based on a given wind direction and mean wind magnitude at 6 [m] of altitude. It also takes into account statistical dependency of wind magnitude on altitude for wind shear. The Dryden wind turbulence model is build for low altitude profile. The required disturbances are obtained by passing white noise through third order shaping filters. Gust model employs ‘1– cosine’ model from the same standard. It is used only at the verification stage to estimate the UAV behavior in presence of random gusts. See Fig. 10.

4.1.1 Wind Model

Side wind is considered as the main disturbance to the system and will therefore be simulated in the wind model. The wind has a 360° (around), and ±180° (up and down) impact on the helicopter but the one with the most influence is a side wind perpendicular to the fuselage coming from the port or starboard side. A portside wind results in a Y force due to fuselage drag, an L moment due to the main rotor dynamics and an N moment due to the tail rotor dynamics. This is of course a simplification of the wind’s influence, but since the controller is to handle worst case scenarios this is considered to be sufficient. The output of the wind model is wind velocity and angular wind velocity as described in Fig. 11.

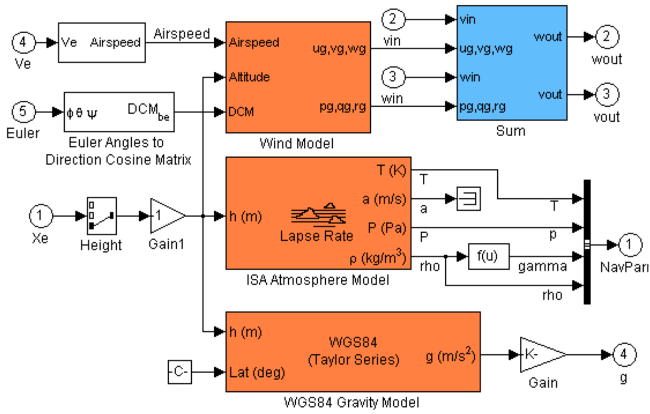

Fig. 10 The environment model.

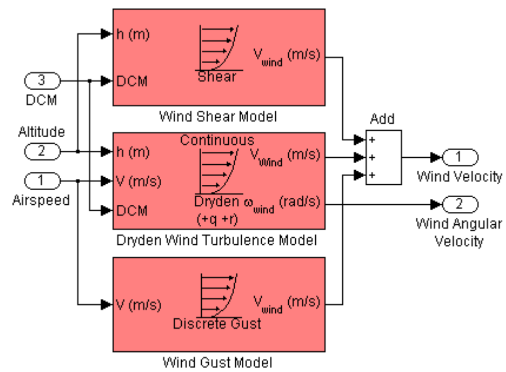

Fig. 11 The wind model.

4.2 Navigation System

The sensor acts as a transducer in the helicopter flight control systems, in that it measures the motion variables and produces output voltages or currents which correspond to these motion variables. There are three sensors aboard the helicopter: an Inertial Navigation System (INS), Global Positioning System (GPS) and one compass. Overviews of sensors model are given in Fig. 12.

The navigation system for the helicopter is based on the onboard inertial system. It is well-known that dead reckoning sensors such as INS have high update rates but the errors are unbound. On the other hand, absolute sensors/position fixed such as GPS have fixed errors even though the update rates are generally low. To earn the benefit while eliminating weaknesses from both types of sensors, a sensor fusion using filtering technique can be designed to integrate INS and GPS measurements.

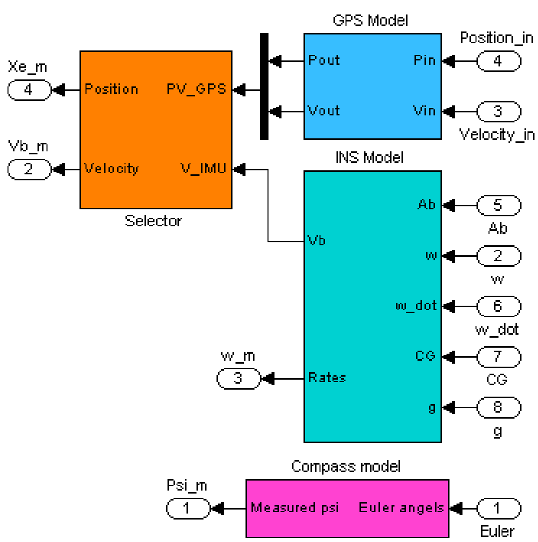

Fig. 12 The navigation model.

Typical GPS signals used for navigation and in the event of missing GPS signals, INS can give aiding data enabling the navigation system to coast along until GPS signal can be re-established. A mathematical model of the INS and GPS has been developed.

4.2.1 Inertial Navigation System (INS)

The INS is given through a block containing an Inertial Measurement Unit (IMU) and Navigation Algorithm. See Fig. 14.The IMU consists of three accelerometers and three gyroscopes which together makes it possible to determine the helicopters change in accelerations and rates in 6-DOF. See Fig. 13.The IMU placement is considered relative to the helicopter gravity center. This will not have any effect on the gyroscope, but the accelerometers will sense a translateral movement as an effect of the rigid bodies Euler rates. In addition the accelerometer will also sense the Earth’s gravity. Therefore the navigation algorithm has to be derived. The navigation algorithm calculates the net acceleration without the effect of gravitation and changing of the helicopter gravity center and doubly integrates the net acceleration to maintain an estimate of the velocity and position of the host vehicle.

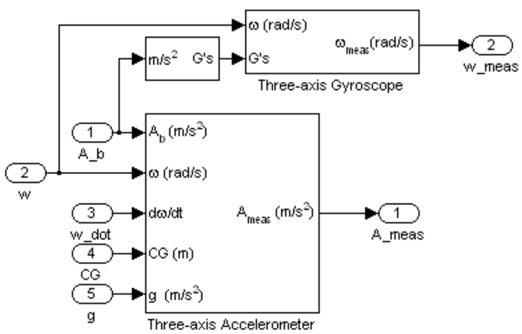

Fig. 13 The IMU model.

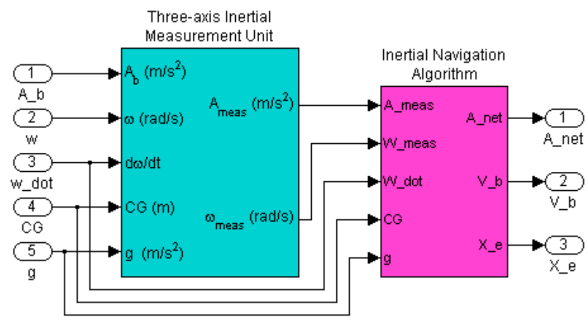

Fig. 14 The INS model.

4.2.2 The GPS Model

INS provides high frequency acceleration and rotation rate data that can be used independent of vehicle models. The equations of inertial navigation are essentially integrators meaning inherent noise and biases in the system lead to unbounded, exponential error growth in time. The desirability of aiding inertial sensors with GPS measurements has long been known. The GPS is a satellite navigation system that gives an accurate determination of position and velocity based on noisy observation of the satellite signals. For the purpose of this simulation, a simple model has been developed to generate the errors of the GPS system and a filter to reduce the noise intensity of the GPS’ output. The models of both components are included in the position and velocity channels. The model has the same structure for both position and velocity but with different parameter values. Fig. 15 shows The GPS model for one channel as simulated in Simulink and the parameters of the GPS model are evaluated in Table 3. The main characteristic of the GPS which have been considered are latency, update rate, accuracy and error dynamics parameter.

The update rate represents the rate at which the position and velocity signals are sent to the receiving processor and is modeled as quantization. The latency is the time delay that occurs between the time the satellite information is received and the time the position or velocity output is sent to the receiver. It is modeled as a pure time delay. The accuracy is the radius of the circle with the origin at the actual position or velocity which contains 50% of the sensors output values. The error of the GPS sensor package is generated as output of a first order linear differential equation with random Gaussian input and initial condition [6].

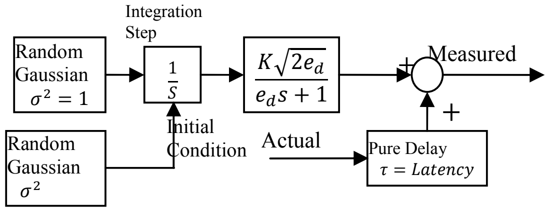

Fig. 15. The GPS model (one channel)

Table 3. The GPS model parameter values

	Position	Velocity
Update Rate	5Hz	5Hz
Latency, τ	0.075 s	0.075 s
Accuracy, K	0.65 ft	0.1 ft
Error Dynamic Parameter, e_d	0.5 sec	2.5 sec

4.2.3 The Compass Model

The compass model act as azimuth indicator and can be used directly by the controller. For the purpose of this simulation, a simple model has been developed to simulate the errors of the true compass by adding an output of a first order linear differential equation with random Gaussian input to the actual azimuth angel of the helicopter model. See Fig. 16. The parameters of the compass model are evaluated in Table 4.

Table 4 The compass model parameter values.

Parameter	Value
Update Rate	5 Hz
Accuracy, K	$\pm 1^0$
Error Dynamic Parameter, e_d	0.5 sec

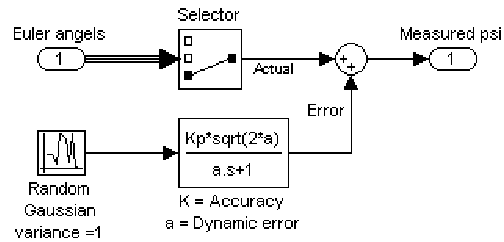

Fig. 16 The compass model.

5. Nonlinear Flight Simulation Model

A full 6-DOF nonlinear model for the helicopter was built in the Matlab/Simulink environment for testing and simulation purposes. The state differential equations of motion that derived in the previous section are utilized in conjunction with an approximation of the aerodynamic forces and moments via component build-up. Fig. 17 shows the complete flight simulation model.

The goal of simulator is to mimic the complex behavior of a helicopter in flight so that it can be used in controller tests without wasting money. A complete sequence of the simulation procedure is shown in Fig. 18.

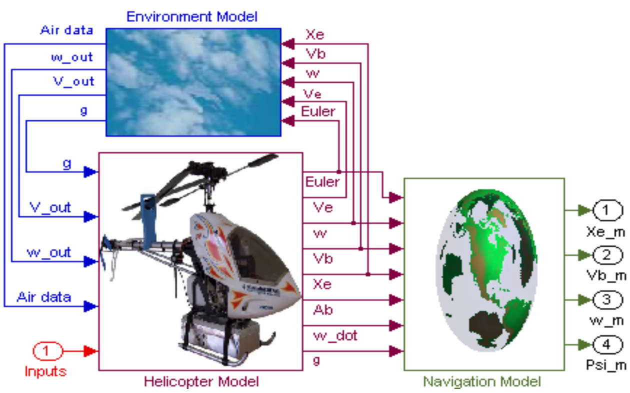

Fig. 17 The flight simulation model.

6. Simulation Results

To verify the nonlinear model, first an analysis of the expected movement of an uncontrolled helicopter in hover is carried out. This analysis is based on causes and effect behavior of the states in the nonlinear model. Thereafter, a simulation of the helicopter model in hover, with no input given, will be performed.

Due to the moment generated by the rotation of the main rotor, the helicopter would rotate about the body z-axis, if the tail rotor not counteracting this moment. And to counteract this moment, the tail rotor produces a force in negative direction of the y-axis. This causes an acceleration of the helicopter in this direction and thereby an increase of the velocity in the same direction. This velocity causes the blades to flap positive lateral, i.e. β_{1s} becomes positive. And due to the cross-couplings of the lateral and longitudinal blade flapping, when the lateral flapping β_{1s} becomes positive, the longitudinal flapping β_{1c} becomes negative. The lateral flapping also makes the helicopter rotate about the body x-axis, i.e. p becomes positive and forces the helicopter velocity along the body y-axis to become positive, that is v becomes positive. The negative longitudinal flapping causes the helicopter to rotate negatively about the body y-axis, i.e. q becomes negative, and thereby giving the helicopter a positive translatory velocity along the body x-axis, that is u becomes positive. This is the cause and effect movement, which must not be confused with being sequential, the hovering helicopter would perform if it is not controlled, illustrated in Fig. 19. In Fig. 20, simulation results for the flapping, translatory velocities, angular velocities and the Euler angels are presented. It can be seen that, at time t = 0, the translatory velocity along the body y-axis becomes negative and the lateral flapping β_{1s} becomes positive. Almost immediately after this, the longitudinal flapping β_{1c} becomes negative. As shown in Fig. 20-(a) the angular velocity p becomes positive almost immediately after the time t = 0 and shortly after q becomes negative. The effect of this can be seen in Fig. 20-(c) as changes in v and u. The negative movement v becomes positive as an effect of p becoming positive and u becomes positive as an effect of q becoming negative. This movement matches the desired movement of Fig. 19 and thereby the qualitative movement of the helicopter is considered to be verified.

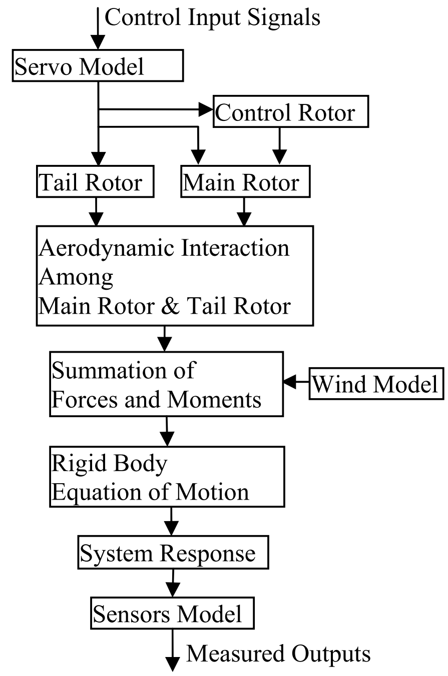

Fig. 18 Simulation procedure.

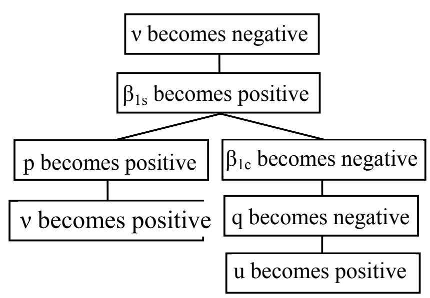

Fig. 19 Illustration of the desired movement of the unstable model during hovering.

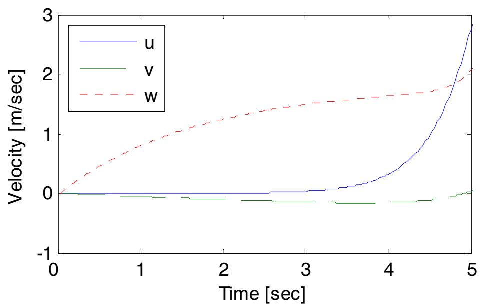

Illustration of the devolvement of the translatory velocities

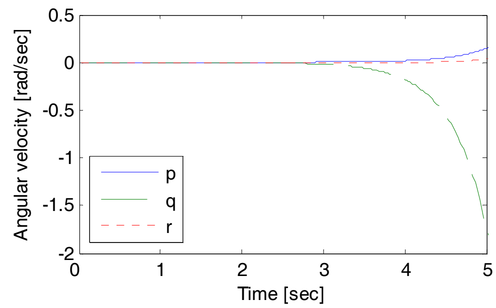

Illustration of the devolvement of the angular velocities

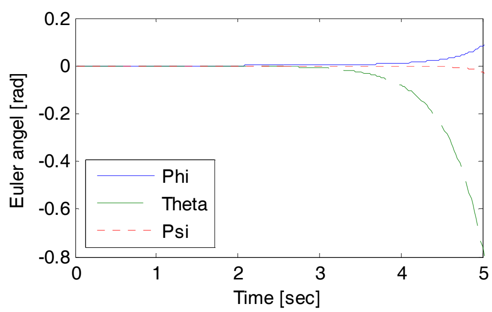

Illustration of the devolvement of the Euler angels

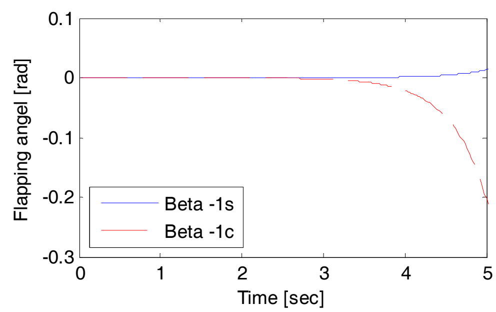

Illustration of the devolvement of the longitudinal and lateral flapping

Fig. 20 Illustration of the devolvement of the states during hovering.

Now, after verifying the nonlinear model in case of no inputs, a simple test for the simulator and analysis of its respective results will be performed. The test presented on Fig. 21 has the purpose of testing the output response to a collective pitch input. In this test the focus is on the thrust response to pitch input and vertical movement. Because of this focus, the coupling from velocities in lateral and longitudinal directions and rotations (p, q and r) has been detached. The first Fig. 21-(a) shows the input signal u_{col}, as it is given a ramp input. The starting value is about 4^0, this is to avoid the thrust/induced velocity problem. Fig. 21-(b) presents the thrust generated from the ramp input. It is not directly dependent on the pitch as one would first imagine. In the beginning of the simulation (first five seconds) the thrust follows the pitch level, but after a while has changed. This change is due to the induced velocity interaction with the increasing body velocity. See Fig. 21-(c).

This interaction can be seen in equation 4. The last Figure in this test presents vertical velocity, keeping in mind that the body z-axis points downwards. The Fig. 21-(c) shows that the helicopter starts off by falling, gradually, as the pitch increased, the helicopter starts to accelerate upwards until about the thrust reaches the equivalent value for the helicopter weight. If aero-dynamical drag from the fuselage had been modeled into the simulator, the result would be that the helicopter reached a terminal velocity, but because this has been omitted the velocity will continue to grow.

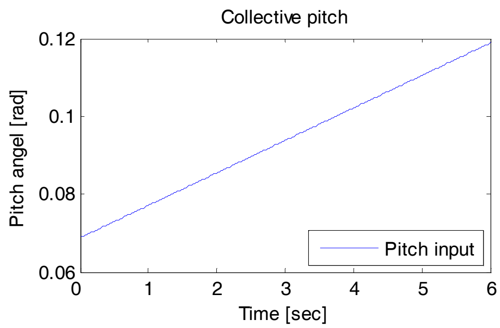

Collective pitch input

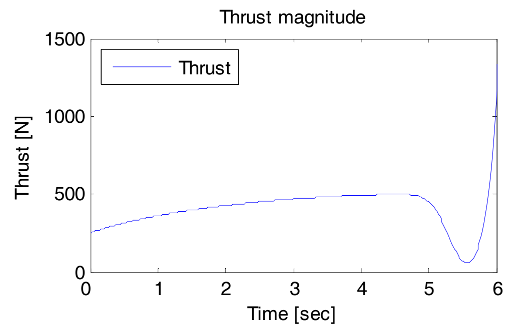

Thrust magnitude

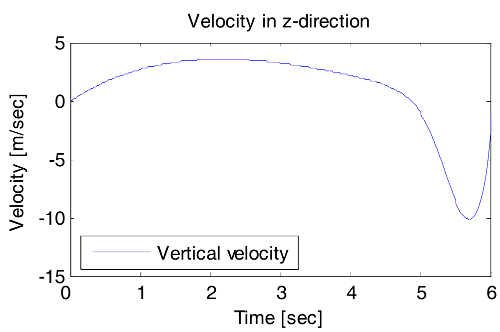

Resulting body velocity in z-Direction

Fig. 21 Pitch - thrust test.

7. Conclusion

The Flight Simulation is an essential part of guidance, navigation, and control design and development. The extensive use of simulation for this purpose generated a design that only needed to be tuned in flight test, saving the program several weeks and perhaps a crash of the aerial vehicle. Also, using the simulation as a tool to correct problems uncovered in flight test saved considerable time as well.

The paper presented a simulation model of "Yamaha R-50" helicopter for the purpose of controller design, stability analysis and controller performance analysis as central element of an autonomous UAV system. The developed helicopter model was simulated in MATLAB/Simulink using S-functions for enhanced performance. The model structure was described and the contribution of the different vehicle components to the global nonlinear dynamic model was discussed. Detailed models for the sensors, servos, and environment data were incorporated in the simulation. The final step was simulating the results using MATLAB/Simulink program when applying no inputs and when applying a ramp input to the collective.

Future work will focus on adjusting and validating model scale helicopter so that it can be used to exploit the particular dynamic characteristics in its whole flight envelope. Extra effort will be placed on studying, developing, and testing advanced control strategies to achieve good performance characteristics in highly demanding maneuvers.

References

[1] M. La Civita, W. Messner, and T. Kanade, "Modeling of small-scale helicopters with integrated first principles and integrated system identification techniques", presented at 58th Forum of American Helicopter Society, Canada, June 2002.

[2] B. Mettler, M.B. Tischler, and T. Kanade, "System identification modeling of a small-scale unmanned rotorcraft for control design", Journal of the American Helicopter Society, January 2002.

[3] R. W. Prouty. "Helicopter Aerodynamics", Philips Publishing Inc. 1986.

[4] F. P. Beer and W. E. Clausen. "Vector Mechanics for Engineers, Dynamics", 7th edition, McGraw-Hill, 2004.

[5] Raymond W. Prouty. "Helicopter Performance, Stability and Control", Krieger Publishing Company, 1990. ISBN 1-57524-209-5.

[6] T. Sudyanto, A. Budiyono, H.Y. Sutarto, "Hardware In-the-loop Simulation for Control System Designs of Model Helicopter," Aerospace Indonesia Meeting, Bandung, July 27, 2005.

[7] The MathWorks, Inc., Simulink user's Guide, USA, 2006.